RESULTS FROM THE HOMESTAKE SOLAR NEUTRINO OBSERVATORY

B. CLEVELAND, T. DAILY, R. DAVIS, J. DISTEL, K. LANDE, C.K. LEE, A. WEINBERGER, P. WILDENHAIN
University of Pennsylvania
Philadelphia, PA 19104

J. ULLMAN
Herbert Lehman College
Bronx, NY 10468

ABSTRACT

The Homestake chlorine detector measures the neutrino flux emitted by fusion reactions in the solar core, via the reaction $\nu_e + {}^{37}Cl \rightarrow e^- + {}^{37}Ar$. The continuous twenty year record of these measurements indicate an average ^{37}Ar production rate of 0.49 ± 0.03 per day corresponding to 2.2 ± 0.3 SNU. The ν_e flux appears to vary with the 11 year solar activity cycle, with higher ν_e fluxes during solar quiet periods and lower ν_e fluxes during solar active periods. When the Homestake data is combined with the Kamiokande results, the region of overlap between the two experiments is for an observed to predicted ^8B neutrino flux ratio of about 0.4 and very little low energy neutrino flux. If the Kamiokande results are corrected for MSW effects, neutral current scatterings by non–electron neutrinos, then both the ^8B and the ^7Be fluxes are about 1/3 of the Standard Solar Model predictions.

INTRODUCTION

For the past twenty years the Homestake chlorine detector, 610 tons of perchloroethylene, has been engaged in measuring the solar neutrino emission from the sun. These observations:

1) provided the first experimental evidence that the Sun generates energy by fusion reactions,
2) showed that the emitted flux of ν_e's is considerably less than expected from the Standard Solar Model,
3) indicated that the observed ν_e flux emitted by the Sun appears to vary with the solar cycle, being larger during solar minimum and smaller during solar maximum.

These observations, together with more recent results from the Kamiokande electron scattering solar neutrino detector and preliminary observations from the Baksan gallium low energy solar neutrino detector, have led to the development of several very interesting theoretical ideas that might account for these observations of reduced ν_e flux and variation of that flux with solar activity cycle. One general feature of all of these suggestions is that the neutrinos have characteristics that have never been observed in terrestrial experiments and that go beyond the standard model of weak interactions.

One of these suggestions, the MSW mechanism, proposes that a resonant conversion of ν_e's into another neutrino flavor occurs within the Sun. A second suggestion, the VVO mechanism, proposes that the neutrino has a small magnetic moment and that during periods of high solar activity there are large magnetic fields within the Sun that extend over sufficiently large regions so that some fraction of electron neutrinos rotate their spin from left–handed to right–handed. These right–handed neutrinos do not interact with matter by the standard V–A weak interaction and thus are not detectable in detectors that utilize inverse beta decay processes. A third suggestion, the transitional magnetic moment, combines the MSW and VVO mechanisms by converting left–handed ν_e's into right–handed muon or tau neutrinos.

In this paper, we will:

1) provide a summary of the last two decades of Homestake data,
2) indicate how these data correlate with solar activity cycle,
3) compare the Homestake data with that from Kamiokande and Baksan, and
4) provide brief summaries of the theoretical explanations of these observations.

THE HOMESTAKE CHLORINE SOLAR NEUTRINO DETECTOR

A description of this detector and tests of its operation has appeared in several earlier papers [1,6,15]. Here we will provide only a brief description, and will focus on the data, its analysis and interpretation. The detector, fig. 1, contains 610 tons of C_2Cl_4. There are 2.17×10^{30} atoms of ^{37}Cl, the operative target, in the detector. The interaction of interest is:

$$\nu_e + {}^{37}Cl \rightarrow e^- + {}^{37}Ar.$$

The ^{37}Ar is removed periodically, about once every 60 days, from the detector by sweeping the detector with a flow of helium. The helium and perchloroethylene are thoroughly mixed by a set of 40 eductors. The perchloroethylene is circulated through the eductors by two large liquid circulation pumps. The circulation established by these pumps insures that liq-

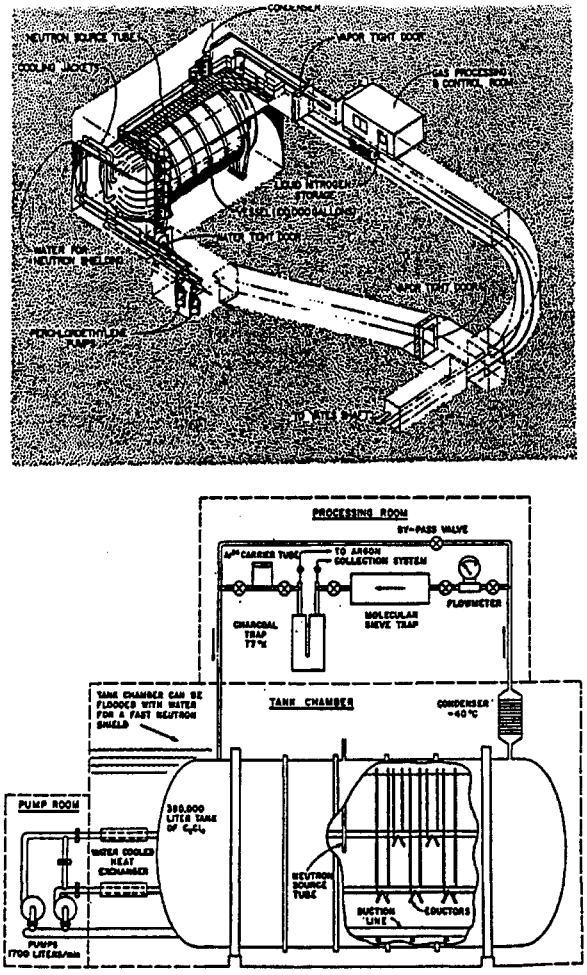

FIGURE 1. A cut away view of the Homestake Perchloroethylene Solar Neutrino Detector. The key features of the detector in addition to the perchloroethylene are, the liquid circulation pumps, the eductors that mix helium sweeping gas and perchloroethylene, the condenser at the exit of the tank that removes most of the perchloroethylene vapor from the exiting gas, the molecular sieve that removes any remaining vapor from the gas, the gas flow meter, heat exchanger and charcoal trap that complete the gas cycle. In addition, there are the reservoirs of ^{36}Ar and ^{38}Ar used to put the "carrier" gas into the tank at the end of each extraction.

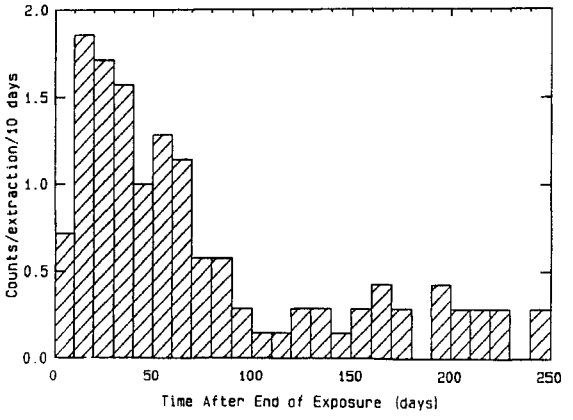

FIGURE 3. The decay time distribution of the data in the 2.82 keV region shown in figure 2. The background after about day 70 is quite flat and at a level of about 0.3 counts per 10 days per extraction. The data of the last year, not shown, is typically a factor of 2 lower in background.

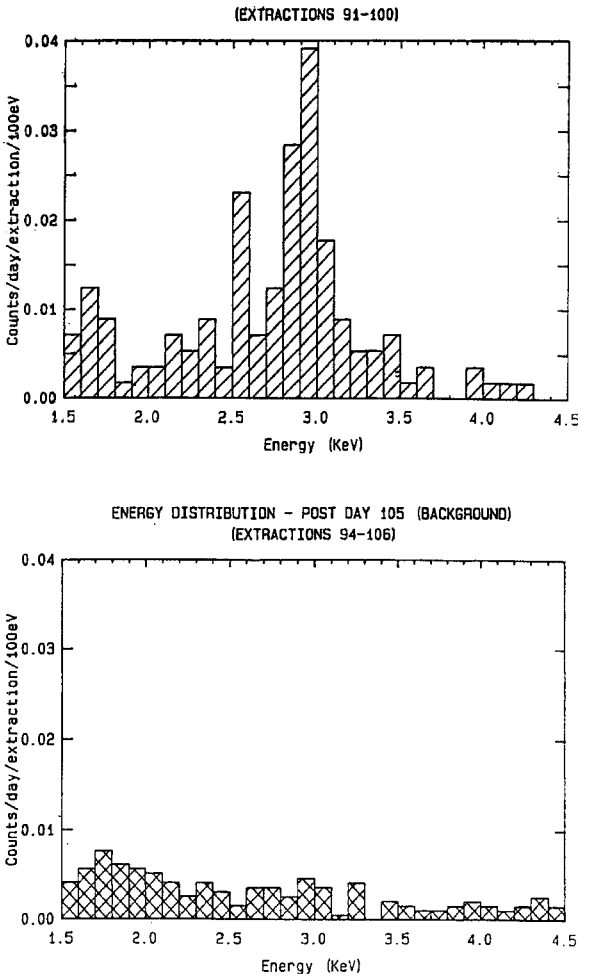

FIGURE 2. (a) The pulse height spectrum of fast rising counts in the proportional counter seen during the first 70 days (two ^{37}Ar half-lives). The peak at 2.82 keV corresponds to the Auger electrons emitted after K orbit electron capture by the nucleus. The data from ten extractions in the period 1987–1989 are used. The plot is normalized to a per extraction basis so that the absolute rates can be utilized.

(b) The same plot as (a) except for the time period after day 105 (after three ^{37}Ar half-lives). This plot is primarily of counter background. There is no evidence of any excess in the 2.82 keV region. The absolute background rates in the region below and above the 2.82 keV window very closely match the rates in these regions in the early time data given in (a) above. If the (b) plot is subtracted from the (a) plot, only a Gaussian distribution centered at 2.82 keV remains.

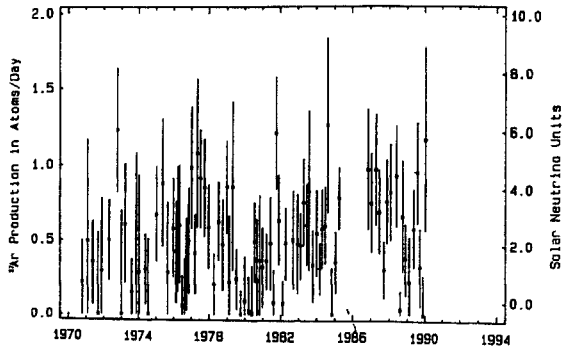

FIGURE 4. Continuous twenty year record of ^{37}Ar production rates in the Homestake chlorine detector. These data indicate an average ^{37}Ar production rate of 0.49 ± 0.03 per day.

uid from all sections of the tank is uniformly swept. The exiting gas then flows through a liquid nitrogen cooled charcoal trap. The argon, which liquifies 10°C higher than nitrogen, is absorbed on the charcoal, while the helium passes through and returns to the perchloroethylene tank[16]. In order to reduce liquid nitrogen consumption, a heat exchanger is used to cool the gas coming into the charcoal trap, while heating the exiting gas.

After each extraction, a few tenths of a cc of either ^{36}Ar or ^{38}Ar are added to the tank. The fraction of this "carrier" gas that is removed during the next extraction is used to determine the extraction efficiency of each run. Extraction efficiencies of 90–95% are obtained, with an average efficiency of 94%. This efficiency is separately measured for each run by carrying out mass spectroscopy of the extracted gas after all the ^{37}Ar counting is completed.

At the end of the extraction cycle the charcoal trap is heated and the trapped gas is swept out by a flow of helium. The extracted gas is purged of all reactive gases by several passes over hot titanium and is separated from radon and any other rare gases by gas chromatography. The remaining argon is then put into a small proportional counter together with some methane.

The filled proportional counter is put into a well shielded enclosure consisting of: (1) a completely closed copper electrostatic shield, followed by, (2) a 30 cm diameter NaI counter with a reentrant well for the counter, followed by (3) paraffin, (4) mercury, and (5) lead shields. Considerable effort is made to control the materials within this shield and avoid any radioactive contaminants. Our average background counting rate within the 25% energy window used for the 2.82 keV Auger signal from the decay of ^{37}Ar is one count per 30 days. This average is for data since 1985, figs. 2 and 3. The best recent runs have backgrounds of one count per 180 days, or two per year.

The proportional counter output pulse is amplified by a preamplifier located inside the copper shield, and followed by a set of external amplifiers. The amplified pulse height and pulse rise time are then digitized and that information together with any coincident signal from the NaI is recorded.

A set of electronic test pulses is sent through the system several times per day and immediately after each proportional counter pulse. These test pulses are injected into the input of the pre–amplifier and thus test the response of the entire amplifier and digitizer system. In addition, a calibration of the proportional counter with an ^{55}Fe source is carried out every 60 days. The ^{55}Fe has a photopeak at 5.95 keV and an escape peak at 3 keV, close to the 2.82 keV peak of Auger electrons from the K orbital electron capture involved in the ^{37}Ar to ^{37}Cl decay.

Each extraction is counted for about one year, about 10 ^{37}Ar half-lives (35 days). The times of occurrence of the selected pulses (fast rising pulses in the K electron capture energy region that are not in coincidence with a NaI pulse) are fit to a two parameter distribution, an exponential decay with a 35 day half-life and a time independent background, fig.3. The fitting process, based on a maximum-likelihood method, was originally designed by Bruce Cleveland [9] and has had recent modifications by Paul Wildenhain. The results of this analysis together with the mean exposure time of each extraction are given in Table 1 and in figure 4. The last displayed extraction, 109, was acquired in March 1990. Our most recent extraction, number 115, was carried out during the first week of April 1991.

There is also an extensive set of plans for calibration of the Homestake ^{37}Cl detector and the proposed ^{127}I detector terrestrial neutrino sources. The ^{8}B sensitivity of both ^{37}Cl and ^{127}I are being checked in a measurement at the beam dump neutrino source at LAMPF and an ^{37}Ar source, monoenergetic ν_e of 0.81 MeV is being considered to verify the ^{7}Be sensitivity of ^{127}I.

RESULTS AND COMPARISON WITH THE STANDARD SOLAR MODEL

From the above data, we obtain an average ^{37}Ar production rate of 0.49 ± 0.03 per day. A small fraction, 10–15%, of this production rate is due to cosmic ray muon interactions. This background rate was originally determined by measuring the depth dependence of the ^{37}Ar with a series of portable 2500 liter perchloroethylene tanks. These were exposed at various mine depths and then brought to our laboratory at the 4850 ft level for processing. By extrapolating from these data, the cosmic ray muon induced background was determined to be 0.08 ± 0.03 ^{37}Ar per day. A second set of measurements, carried out jointly with the late Edward Fireman, used a KOH target to look for muon induced ^{39}K to ^{37}Ar transitions[2]. These measurements, extended to the full depth of the Homestake experiment, give a slightly smaller cosmic ray production rate, 0.05 ^{37}Ar per day (preliminary analysis). The local cosmic ray muon flux is continually monitored by a scintillation hodoscope that surrounds the perchloroethylene tank[3].

The conversion of the ^{37}Ar production rate to a measure of the solar neutrino flux requires subtraction of the cosmic ray induced ^{37}Ar rate. Because the uncertainty in the cosmic ray background is comparable to the uncertainty in the total measurement, the error in the solar neutrino flux measurement is appreciably increased. Given the small rates involved, we do not see a simple way to reduce the uncertainty in the cosmic ray induced background.

Table 1

RUN	SIGNAL	MEAN DATE	SUN SPOTS	RUN	SIGNAL	MEAN DATE	SUN SPOTS
18	0.22±0.28	70.780	86.6	66	0.36±1.25	80.836	155.0
19	0.49±0.34	71.098	79.0	67	0.32±0.27	80.999	174.4
20	0.35±0.28	71.383	57.5	68	0.36±0.19	81.218	135.5
21	0.00±0.56	71.675	50.2	69	0.48±0.31	81.448	90.9
22	0.29±0.49	71.885	63.2	70	0.08±0.22	81.616	158.7
24	0.50±0.27	72.311	63.2	71	1.21±0.37	81.770	162.4
27	1.23±0.41	72.765	61.3	72	0.64±0.30	81.913	150.1
28	0.00±1.17	73.002	43.4	73	0.08±0.15	82.136	163.6
29	0.61±0.40	73.218	46.0	74	0.48±0.24	82.305	122.0
30	0.15±0.22	73.581	25.6	75	0.50±0.33	82.719	118.8
31	0.51±0.58	73.873	23.9	76	0.48±0.33	82.968	127.0
32	0.28±0.65	74.023	27.6	77	0.46±0.22	83.137	51.0
33	0.31±0.24	74.398	39.5	78	0.75±0.29	83.305	80.7
35	0.00±0.51	74.553	55.8	79	0.60±0.27	83.471	91.1
36	0.67±0.32	75.028	18.9	80	0.82±0.52	83.606	71.8
37	0.88±0.42	75.370	9.0	81	0.33±0.24	83.812	55.8
38	0.28±0.48	75.654	39.7	82	0.55±0.29	84.028	57.0
39	0.58±0.33	75.978	7.8	83	0.31±0.17	84.193	83.5
40	0.42±0.34	76.134	4.3	84	0.58±0.26	84.316	69.7
41	0.57±0.42	76.232	21.9	85	0.60±0.26	84.487	46.1
42	0.61±0.93	76.340	12.4	86	1.26±0.57	84.624	25.5
43	0.06±0.20	76.485	12.2	87	0.00±0.26	84.847	22.8
44	0.05±0.32	76.625	16.4	88	0.29±0.17	85.060	16.5
45	0.34±0.31	76.732	13.5	89	0.72±0.26	85.268	16.2
46	0.49±0.35	76.868	5.2	90	0.00±1.67	86.677	3.8
47	0.98±0.40	77.020	16.4	91	0.98±0.39	86.875	15.2
48	0.41±0.27	77.221	8.7	92	0.75±0.33	87.058	10.4
49	1.08±0.48	77.345	18.6	94	0.97±0.36	87.305	39.6
50	0.91±0.32	77.526	21.4	95	0.69±0.28	87.479	17.4
51	0.85±0.32	77.754	43.8	96	0.30±0.19	87.720	33.9
52	0.59±0.28	77.982	43.2	97	0.76±0.28	87.889	39.9
53	0.20±0.20	78.279	99.7	98	0.82±0.32	88.086	50.0
54	0.63±0.26	78.523	70.4	99	0.94±0.85	88.237	76.2
55	0.47±0.31	78.755	125.1	100	0.93±0.33	88.415	80.0
56	0.85±0.31	78.980	122.7	101	0.04±0.13	88.604	111.6
57	0.22±0.45	79.110	137.5	102	0.53±0.38	88.755	125.1
58	0.85±0.56	79.304	101.5	103	0.36±0.24	88.907	125.1
59	0.24±0.20	79.517	142.2	104	0.08±0.35	89.121	165.1
60	0.00±0.16	79.746	188.4	105	0.57±0.26	89.378	138.5
61	0.09±0.30	79.991	176.3	106	0.96±0.33	89.580	161.6
62	0.02±0.23	80.211	126.2	107	0.48±0.26	89.721	176.7
63	0.00±0.33	80.391	179.9	108	0.22±0.19	89.889	173.0
64	0.49±0.27	80.548	136.3	109	1.20±0.36	90.043	177.3
65	0.22±0.43	80.687	155.0				

Sunspot Numbers from Solar-Geophysical Data prompt reports published by National Oceanic and Atmospheric Association National Geophysical Data Center, Boulder, Colorado

The measured solar neutrino flux, 2.1 ± 0.2 SNU, provided the first experimental evidence that fusion reactions are occurring in the Sun. However, this observed rate is about 1/3 of that predicted for this detector by the Standard Solar Model. Among recent calculations of the predicted rates for the chlorine detector are those of Bahcall and Ulrich of 7.9 ± 2.6 (3σ) SNU[4], Turch-Chieze, et. al. [5], and Sackman, Boothroyd and Fowler, 7.7 SNU [18]. The difference between observed and predicted fluxes has attracted considerable theoretical interest and will be discussed below.

IS THERE VARIATION IN THE SOLAR NEUTRINO FLUX?

A general characteristic of the data is that the measured ^{37}Ar production gradually increased during the period of the late 1970's and then abruptly dropped around 1980. Following that sudden drop, the period of the 1980's again saw a gradual increase of the ^{37}Ar production rate culminating in a rate in the late 1980's very similar to that in the late 1970's. Around 1989, the rate again dropped.

Beginning in the early 1980's, a number of analyses of this rate variation and suggestions of possible mechanisms occurred. The pattern of these flux variations is similar to that of the solar activity cycle, suggesting that the solar ν_e flux varied inversely with the solar cycle. The best determined measure of the solar cycle is the number of visible sunspots. Records of sunspots date back to the 17th century and are quite complete for the past 200 years. Other, more recently measured characteristics of solar cycle seem to follow the same general time variation as do the sunspot numbers; e.g. the solar luminosity, the p-mode acoustical spectra, and the solar diameter.

In figure 5, we compare the ^{37}Ar production rate with the number of sunspots observed during the same time interval. It is clear that when the sunspot number is small, the ^{37}Ar is high and when the sunspot number is large, the ^{37}Ar is small. In figure 6, we combine these data into five points. A correlation is rather apparent. This observation has been made by a number of authors, with varying explanations for this correlation. It is clear that improved statistics are very desirable and that a higher counting rate experiment is called for.

The Homestake data has been analysed rather extensively by a large number of groups [7, 19, 20, 21, 22, 23, 24, 25, 26, 27, 28, 29, 30, 31, 32, 33, 34, 35, 36, 37, 38]. These analyses were made as the data evolved. The questions addressed were: did the data set arise from a constant flux of neutrinos and, if not, did the variations that arose correlate with solar or other astronomical phenomena? The consensus in these analyses is that there is an apparent

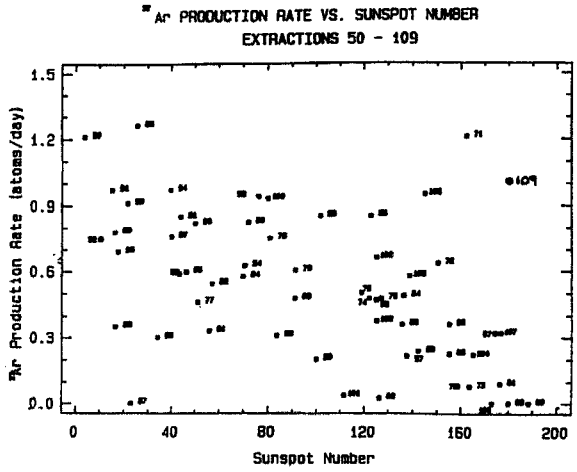

FIGURE 5. The argon production vs. sunspot number for each of the extractions since 1978. There is a clear cut relationship; when the sunspot number is high, the argon production is low and when the sunspot number is low, the argon production is high.

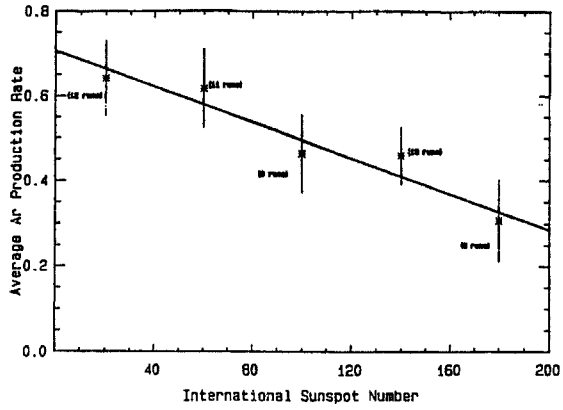

FIGURE 6. The data of figure 5 is statistically combined into five points and the best fit line is shown.

anti-correlation of the ^{37}Ar production rates observed by the Homestake experiment with the solar activity cycle in the period 1977–1990. As is well known, the galactic cosmic ray intensity also anti–correlates with the solar cycle (e.g. see [39]). However, we do not expect this variation in cosmic rays to effect the ^{37}Ar rate since the muon induced background is very small and since, 3 TeV muons, those that reach our detector, are not significantly effected by the solar cycle. Nor would the neutrinos produced by galactic cosmic rays in the earth's atmosphere be expected to play a role [40].

We are thus faced with two problems, why is the observed ν_e flux less than that predicted by the standard solar model and why does the observed ν_e flux vary with solar cycle?

SOLAR NEUTRINO TIME VARIABILITY AND FLAVOR CHANGE

There are two general possible sources for time variation of the detected solar neutrino flux: either a time variation in the fusion reaction rates in the solar core or time variable absorption or interaction processes that involve neutrinos as they travel through the Sun. We are not aware of any models that predict a short, 10 year time variation in the nuclear fusion reactions in the solar core. Indeed, it is generally assumed that the time scale for variations in the solar core must be of the order of 10^7 years. However, one must bear in mind that the solar activity cycle is not understood, nor are other periodicities in solar phenomena.

Several mechanisms have been suggested for changing the state of neutrinos as they pass through the Sun. The first of these, the MSW (Mikhe'ev, Smirnov, Wolfenstein) mechanism [12], proposed that ν_e's undergo a resonant transition to another neutrino state, either muon or tauon, in a region of the Sun where the effective masses of the two neutrino states are degenerate. In order for this process to operate it is necessary that a lepton flavor changing interaction exist. No such interaction has been observed in earth based experiments or in cosmic ray neutrino observations.

The effect of the MSW process is to attenuate the ν_e efficiently by converting them to more massive neutrino states. These heavier neutrinos have too little energy to drive nuclear transformation processes, since a muon or a tauon must be produced in the final state, and thus are not detectable in our detector. The MSW mechanism was originally proposed to explain the large difference between the observed and predicted neutrino fluxes. It does not naturally have any time variable transformation rate [41].

A second idea, suggested by Voloshin, Vysotskii, and Okun, [13], is that the neutrino has an anomalously large magnetic moment, 10^{-11} μ_B. It is further assumed that during the solar active period the internal magnetic fields in the Sun are several kilogauss and extend over 10^9cm. Under these conditions, the left–handed ν_e can have their spins rotated and become right–handed particles. Right–handed neutrinos will not interact by the conventional weak interactions, V–A, and thus may not be detectable. The VVO suggestion first arose to explain the flux decrease in 1980. They pointed out that the sharp dips in the 1980 data corresponded to the times during the year when the earth was furthest above or below the solar equator, around March 5 or September 5. It is assumed that during the solar active periods the magnetic fields in the Sun are toroidal, with opposite directions in the northern and southern solar hemispheres, and with no magnetic field along the solar equator. Thus, the largest flux reductions might be expected when the earth is at the extremes of solar magnetic latitude and the smallest reductions would occur when the earth is aligned with the solar magnetic equator. However, the solar magnetic and rotational equators do not necessarily coincide.

Lim and Marciano and Akhmedov [14] merged the two above ideas into a third suggestion, invoking a transitional magnetic moment. In this model, there is a simultaneous magnetic moment flip and MSW flavor change, which convert a left–handed ν_e into a right–handed ν_μ, or ν_τ (anti–neutrinos in the Majorana case). Both magnetic moment suggestions could give rise to the observed anti–correlation of chlorine detector count rate with solar cycle activity (as measured by the sunspot number).

The MSW process may depend on neutrino energy and thus can result in a distortion of the neutrino energy spectrum. Bahcall and Bethe [42] suggest that the parameters of MSW that correctly describe solar neutrino effects supress low energy neutrinos and leave the high energy ones virtually unchanged. The VVO mechanism is probably energy independent and should effect all neutrino energies equally.

It is thus desirable to determine the neutrino flux as a function of energy. The chlorine detector is sensitive to two neutrino fluxes, ^{8}B and ^{7}Be. However, with only one measurement it is not possible to determine separately the reduction factors for these two fluxes. Instead, in figure 7, we show the locus of all possible fits to the data. On the horizontal axis we have the ratio of the observed to predicted ^{8}B neutrino flux and on the vertical axis the observed to predicted low energy neutrino flux. For example, it is possible to find solutions which maximize the high energy flux at the price of no low energy neutrinos or solutions which allow the full low energy flux with extremely little ^{8}B neutrino flux. Another experiment

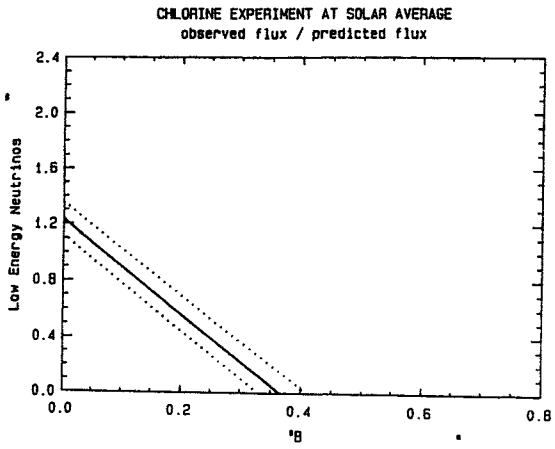

FIGURE 7. The locus of all possible solar neutrino fluxes that fit the Homestake data. On the horizontal axis we have the ratio of the observed to predicted ^{8}B neutrino flux and on the vertical axis the observed to predicted low energy neutrino flux.

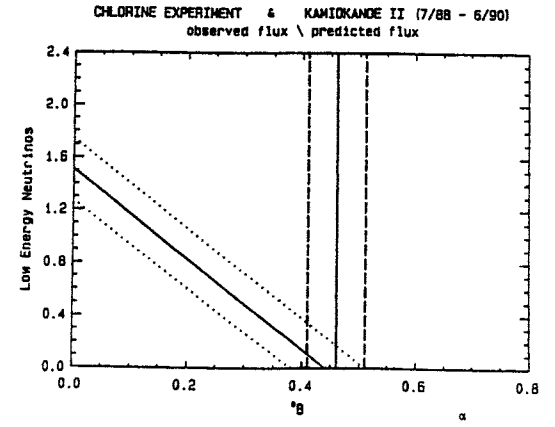

FIGURE 8. The same ratios of observed to predicted fluxes for ^{8}B and low energy neutrinos as in figure 7, but only use the Homestake data that corresponds to the period when Kamiokande was observing. The Kamiokande results appear as a vertical band since only high energy neutrinos are involved. The region of overlap between the two experiments is for an observed to predicted ^{8}B neutrino flux ratio of about 0.4 and very little low energy neutrino flux.

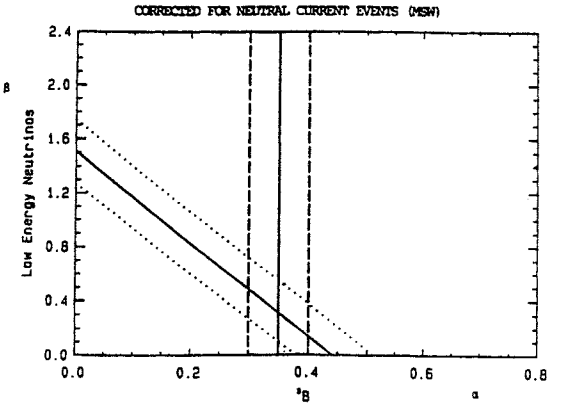

FIGURE 9. The same overlap of Homestake and Kamiokande results, as figure 8, except the Kamiokande signal has now been corrected for neutral current interactions of non-electron neutrinos as per the MSW model. The resulting solution now suggests that the ^{8}B and the ^{7}Be electron neutrino fluxes are now about 1/3 of that predicted by the SSM.

is required to permit the separate determination of the fluxes from these two sources.

COMPARISON OF HOMESTAKE DATA WITH THAT OF OTHER DETECTORS

By combining our observations with those from other detectors, Kamiokande and Baksan, we can determine the fluxes from the various neutrino sources in the Sun, ^{8}B decay, $e^- + {}^7$Be and P–P fusion, and so see if there is any energy dependence of the ν_e flux attenuation.

During the period 1987–90, the Kamiokande II water Cerenkov detector measured solar neutrino flux via elastic scattering from electrons. Since the Kamiokande threshold for scattered electrons was high, about 9 MeV for the first half of this period and 7 1/2 MeV for the second half, the detector is sensitive only to neutrinos from ^{8}B decay. The observed rate is 0.46 ± 0.08 of that predicted by Bahcall and Ulrich and shows less than 30% time variation [11].

In figure 8, we show the same ratios of observed to predicted fluxes for ^{8}B and low energy neutrinos as in figure 7, but only use the Homestake data that corresponds to the period when Kamiokande was observing. The Kamiokande results appear as a vertical band in figure 8, since only high energy neutrinos are involved. The region of overlap between the two experiments is for an observed to predicted ^{8}B neutrino flux ratio of about 0.4 and very little low energy neutrino flux.

Even if ν_e's are converted into other flavors, these converted neutrinos may still produce a signal, albeit diminished, in the Kamiokande detector, since these other flavor neutrinos can scatter from electrons via neutral currents. However, these converted neutrinos will not induce ^{37}Cl to ^{37}Ar transitions. Thus, the Kamiokande detector will detect a different neutrino flux than will the Homestake detector. The correction for this effect is model dependent and so cannot be completely specified. This fact is important to bear in mind when comparing the signal rates of different kinds of solar neutrino detectors.

As an example, we will assume that the MSW model applies and that we can ignore any variations of neutrino resonant transitions over the ^{8}B decay spectrum. In that case, we find that of the 0.46 of the SSM signal reported by Kamiokande, 0.35 is due to charged current scattering of ν_e and 0.11 is due to neutral current scattering of all neutrino species. In figure 9, we show the same overlap of Homestake and Kamiokande results, except the Kamiokande signal has now been adjusted to center at 0.35 of the predicted SSM. The resulting solution now suggests that the ^{7}Be ν_e flux is also about 1/3 of that predicted by

the SSM.

A third detector, the Baksan gallium solar neutrino detector has recently become operational. The ^{71}Ga to ^{71}Ge transition has a very low threshold, 233 keV, and thus can be driven by the P–P fusion neutrinos. The fluxes of the Standard Solar Model predict that a gallium detector should see a signal of 132 SNU, of which more than half, 70 SNU, come from the P–P neutrinos, 34 SNU from the ^{7}Be neutrinos, 14 SNU from the CNO cycle and 14 SNU from the ^{8}B neutrinos. The observations for the first half of 1990, reported at Neutrino '90, are that the observed signal is less than 70 SNU. After subtracting the contributions to the signal from ^{8}B, ^{7}Be and CNO, as determined by the MSW solution of 20 SNU, we are left with an upper limit of 50 SNU. Again, we are left with a considerably reduced solar ν_e signal. As further data is obtained from both the Baksan and GALLEX gallium detectors, a clearer picture of the P–P neutrino flux will emerge. Present indications are consistent with significant reductions of ν_e flux over the entire solar neutrino spectrum.

The next several years present a most unusual opportunity in solar neutrino investigations, the simultaneous operation of four different detectors, Homestake, Kamiokande, and the two gallium detectors, Baksan and GALLEX. Being able to use all these data simultaneously will permit far more complex fits of the solar neutrino emission and thus allow much better determination of the characteristics of the emitted neutrinos and therefore of the mechanisms operating in the Sun that modify neutrino flavors and states.

There is also an extensive set of plans for calibration of these solar neutrino detectors using terrestrial neutrino sources. The ^{8}B sensitivity of both ^{37}Cl and the future Homestake ^{127}I detector are being checked in a measurement at the beam dump neutrino source at LAMPF and an ^{37}Ar source, monoenergetic ν_e of 0.81 MeV is being considered to verify the ^{7}Be sensitivity of ^{127}I.

REFERENCES

1. Davis, Jr., R., BNL50879, *The Status and Future of Solar Neutrino Research*, 1, (1978), G. Friedlander, Editor.
2. Fireman, E.L., Cleveland, B.T., Davis, Jr., Rowley, J.K., *A.I.P. Conference Series* **126**, 22 (1984), Cherry, M.L., Fowler, W.A. and Lande, K., Editors
3. Kieda, D. et. al., *Ap.J.* (1990) to be published.
4. Bahcall, J.N., *Rev. Mod. Phys.* **50**, 881 (1978); Bahcall, J.N. et al, *Rev. Mod. Phys.* **54**, 767 (1982); Bahcall, J.N. and Ulrich, R., Rev. Mod. Phys. **60**, 297 (1988); Filippone, B.W. and Schramm, D.N., *Astrophys. J.* **253**, 393 (1982).
5. Turck-Chieze, S., Cahen, S., Casse, M. and Doom, C., *Astrophys. J.* **335**, 415 (1988).
6. Rowley, J.K., Cleveland, B.T., Davis, Jr., *A.I.P. Conference Series* **126**, 22 (1984), Cherry, M.L., Fowler, W.A. and Lande, K., Editors.
7. Haubold, H.J. and Gerth, E., *Astron. Nacht.*, **304**, 299 (1983).
8. Ferraz-Mello, S., *Ap. J.* **86**, 619 (1981). We are indebted to Dr. Emilia P. Belserene for supplying us with the DCTFT computer program used in these analyses.
9. Cleveland, B.T., *Nucl. Inst. Meth.*, **214**, 451 (1983).
10. U. S. Department of Commerce (National Oceanic and Atmospheric Administration) 1989, *Solar-Geophysical Data* and earlier issues of this series.
11. Hirata, K.S. et al (The Kamiokanka II Collaboration), *Phys. Rev. Lett.* **63**, 16 (1989), **65**, 1297 (1990), **65**, 130 (1990).
12. Wolfenstein, L., *Phys. Rev.* **D17**, 2369 (1978), Mikhe'ev, S.P. and Smirnov, A. Yu., *Soviet J. Nucl. Phys.* **42**, 913 (1985); *Nuovo Cimento* **9C**, 17 (1986), see Soviet Physics., Gelb, J.M. and Rosen, S.P., *Phys. Rev.* **D34**, 969 (1986), Bethe, H.A., *Phys. Rev. Lett.* **56**, 1305 (1986), Uspehki **30**, 759 (1987), Kuo, T.K. and Pentaleone, J. *Rev. Mod. Phys.* **61**, 937 (1989); Barger, V., Phillips, R.J.N. and Whisnant, K., *Phys. Rev.* **D43**, 1110 (1991).
13. Voloshin, M.B., Vysotskii, M.I. and Okun, L.B., *Soviet J. Nucl. Phys.* **44**, 440 (1986); *Soviet Phys. JETP* **64**, 446 (1986).
14. Lim, C.S. and Marciano, W.J., *Phys. Rev.* **D37**, 1368 (1988); Akhmedov, E. Kh., *Phys. Lett.* **213B**, 64 (1988) and *Soviet J. Nucl. Phys.* **48**, 382 (1988); Sivaram, C., *21st International Cosmic Ray Conference*, Vol. 7, 176 (1990).
15. Bahcall, J.N. and Davis Jr., R., *Science* **191** (1976).
16. Davis Jr., R., Harmer, D.S. and Hoffman, K.C., *Phys. Rev. Lett.* **20**, 1205 (1968).
17. Wolfendale, A.W., Young, E.C.M. and Davis, R., *Nature (Phys. Sciences)* **238**, 1301 (1972); Cassidy, G.L., *Proc. 13th Int. Conf. on Cosmic Rays* **3**, 1958 (1973).
18. Sackmann, I.-J., Boothroyd, A.I., and Fowler, W.A., *Ap.J.* **360**, 727 (1990).
19. Ehrlich, R., *Phys. Rev.* **D18**, 2323 (1978), **D25**, 2282 (1982).
20. Haubold, H.J. and Gerth, E., *Solar Phys.* **127**, 347 (1990).

21. Bazilevskaya, G.A., Mukhamedzhanov, A.M.–A., Nikol'skii, S.I., Stozhkov, Yu.I. & Charakhchyan, T.N., *Soviet J. Nuclear Phys.* **39**, 543 (1984).
22. Gavrin, V.N. and Kopylov, A.V., *Soviet Astron. Lett.* **10**, 62 (1984).
23. Lanzerotti, L. and Raghavan, R.S., *Nature* **293**, 122 (1981).
24. Bahcall, J.N., Field, G.B. and Press, W.H., *Ap. J.* **320**, L69 (1987).
25. Subramanian, A. and Lal, S., *Astron. Nachr.* **308**, 127 (1987); with Yvas, P., *Astron. Nachr.* **309**, 363 (1988).
26. Raychaudhuri, P., *Solar Phys.* **104**, 415 (1986).
27. Wilson, R.M., *Solar Phys.* **112**, 1 (1987).
28. Attolini, M.R., Cecchini, S., Castagnoli, G.C. and Galli, M., *Astro. Lett. and Communications* **27**, 55 (1988).
29. Baltz, A.J. and Weneser, *J. Nucl. Phys.* **A505**, 67 (1988); with Rowley, J.K., Brookhaven Natl. Lab. Report BNL–43625 (1989).
30. Nunokawa, H. and Minakata, H., *Int. J. Mod. Phys.*, to be published, 1991.
31. Bieber, J.W., Seckel, D., Stanev, T., Steigman, G., *Nature* **348**, 407 (1990).
32. Krauss, L.M., *Nature*, **348**, 403 (1990).
33. Filippone, B.W., Vogel, P., *Phys. Lett.* **B246**, 546 (1990).
34. Fiorentini, G. and Mezzorani, G., *Phys. Lett.* **B253**, 181 (1991).
35. Sakuri, K., *Proc.21st Int. Cosmic Ray Conf.* **7**, 172, Adelaide, Australia (1990), *Nature* **278**, 146 (1984), *Space Science Rev.* **38**, 243 (1989).
36. Dorman, L.I. and Wolfendale, A.W., submitted to J. Phys. G.
37. Gavryuseva, E.A., Gavryusev, V.G. and Rosljakov, A.G., Inst. Nucl. Phys., Moscow, preprint P–0672.
38. Bahcall, J.N., Press, W.H., *Ap.J.* **370**, 730 (1991).
39. Akasofu, S.–I., Olmsted, C. and Lockwood, J.A., *J. Geophys. Res.* **A93**, 8735 (1988).
40. O'Brien, K. and de la Zerda, A., *Nature* **330**, 353 (1987).
41. Baltz, A. and Weneser, *J. Nucl. Phys.* **A505**, 67 (1989).
42. Bahcall, J.N. and Bethe, H.A., *Phys. Rev. Lett.* **65**, 2233 (1990).